Sevoflurane exerts protective effects on liver ischemia/reperfusion injury by regulating *NFKB3* expression via miR-9-5p

XINGZHI LIAO[1,2], SIQI ZHOU[3], JIAN ZONG[1] and ZHIPING WANG[1]

[1]Department of Anesthesiology, The Affiliated Wuxi People's Hospital of Nanjing Medical University, Wuxi, Jiangsu 214023; [2]Department of Anesthesiology, The 101st Hospital of Chinese People's Liberation Army, Wuxi, Jiangsu 214044; [3]Department of Gastroenterology, Nanjing Medical University Affiliated Drum Tower Clinical Medical College, Nanjing Medical University, Nanjing, Jiangsu 210008, P.R. China

Received April 4, 2018; Accepted November 27, 2018

DOI: 10.3892/etm.2019.7272

Abstract. Hepatic ischemia/reperfusion (IR) injury is a critical contraindication of hepatobiliary surgery and results in severe liver damage. It is imperative to identify underlying pathophysiological mechanisms. In the current study, a rat model of liver IR was established to explore the mechanisms of sevoflurane during surgical intervention on IR. The detection of cytokines was performed using ELISA and reverse transcription-quantitative polymerase chain reaction and western blot assays were used to detect mRNA and protein expression levels, respectively. The target protein of microRNA (miR)-9-5p was identified by *in vitro* luciferase reporter assay. Cell apoptosis was detected by Annexin-V/propidium iodide and TUNEL staining assays. The results demonstrated that sevoflurane exerted protective effect against liver IR. Sevoflurane administration ameliorated a cytokine storm by decreasing serum levels of interleukin (IL)-1 and -6 and tumor necrosis factor (TNF)-α, and improved liver function was determined. IR-induced damage was mediated by an increase in transcription factor p65 expression and activation of the nuclear factor (NF)-κB signaling pathway, which were suppressed by sevoflurane treatment. *In situ* analysis predicted that *NFKB3*, encoding for p65, may be targeted by miR-9-5p and the hypothesis was verified by *in vitro* reporter assays using wild type and mutant sequences of the *NFKB3* 3'-untranslated region. Furthermore, pretreatment of hepatic tissue with a miR-9-5p mimic inhibited IR-associated injury as suggested by the decrease in the Suzuki score and decreased serum levels of TNF-α, IL-1 and IL-6. The results indicated that sevoflurane protected the liver from IR injury by increasing miR-9-5p expression and miR-9-5p may be a potential treatment target in IR.

Correspondence to: Dr Zhiping Wang, Department of Anesthesiology, The Affiliated Wuxi People's Hospital of Nanjing Medical University, 299 Qingyang Road, Wuxi, Jiangsu 214023, P.R. China
E-mail: zpwang_wx@163.com

Key words: ischemia/reperfusion injury, microRNA-9-5p, sevoflurane, volatile anesthetic, nuclear factor-κB

Introduction

Liver ischemia/reperfusion (IR) is a major cause of liver damage (1,2). IR occurs following tissue resection, hemorrhagic shock or transplantation surgery, when tissue damage occurs due to transient hypoxia and subsequent restoration of blood flow (3,4). Managing IR is an important factor in hepatobiliary surgery (5). IR affects liver function and creates postoperative complications in the cardiovascular system (6).

Molecular mechanisms underlying IR have been extensively explored (7). Various studies have indicated that IR is associated with lactate accumulation, acidosis, depletion of ATP, reactive oxygen species generation and resulting oxidative stress, neutrophil activation and calcium overload (8-11). However, the full pathophysiological process of IR is not completely known.

Interestingly, use of volatile anesthetics can prevent tissue damage by regulating hepatic blood flow following liver ischemia (12-14). Sevoflurane, an inhalation anesthetic, functions as a bronchodilator via regulating calcium homeostasis (15). Sevoflurane renders protection form reperfusion injury during thoracic surgery (16). In fact, sevoflurane has been demonstrated to have a protective effect against liver IR in mouse models (17,18).

IR induces the activation of the nuclear factor (NF)-κB signaling pathway, which mediates IR-associated tissue injury and sevoflurane ameliorates this NF-κB activation (18). It was suggested that sevoflurane exerts its effects by downregulating miR-200c expression (17). However, it remains unknown how sevoflurane regulates the activation of the NF-κB signaling pathway. The objective of the current study was to establish an IR rat model and to verify the mechanism by which sevoflurane regulates the activation of the NF-κB signaling pathway. The results suggested that sevoflurane induced microRNA (miRNA or miR)-9-5p, which targets *NFKB3*, encoding for transcription factor p65, and mitigated the effects of IR.

Materials and methods

Animals, surgery and experimental intervention. The study was approved by the Institutional Animal Care and Use Committee

of Wuxi People's Hospital Affiliated to Nanjing Medical University (Wuxi, China). A total of 36 male Sprague-Dawley rats (Beijing Vital River Laboratory Animal Technology Co., Ltd., Beijing, China) aged 8 weeks and weighing 285±30 g were housed at 22±1˚C with 50±10% relative humidity at 12-h light/dark cycles and with free access to water and food. The animals were randomly assigned to six groups (n=6 rats/group): Control (sham), IR, IR+sevoflurane, IR+miR-9-5p mimic group, IR+miR-9-5p antagomir group, IR+sevoflurane+miR-9-5p antagomir group. All rats were anesthetized using an intraperitoneal injection of sodium pentobarbital (1%; 40 mg/kg body weight) and rats in sevoflurane groups were then treated with sevoflurane (3%; AbbVie Inc., Chicago, IL, USA) at a controlled flow rate (2 l/min) for the full duration of the surgical intervention. Midline laparotomy was performed to reveal the hepatic artery and portal vein for subsequent occlusion. Liver ischemia was induced by ligating the hepatic artery, portal vein and bile duct for 1 h and reperfusion was performed by removing the clamping for 2 h. Post-surgery liver tissue samples were collected and snap frozen in liquid nitrogen or fixed in 4% paraformaldehyde for 24 h at 25˚C. Fixed tissues were used for immunohistochemistry analysis and were stained with hematoxylin/eosin (H&E), including staining with 0.5% hematoxylin for 5 min followed by 0.5% eosin for 1 min at 25˚C. The Suzuki score (criteria, 0-4) assesses liver damage and was used for grading of hepatic IR injury based of the fixed tissues (19). Venous blood samples (5 ml) were collected at 4 h post reperfusion, centrifuged (5 min; 4,000 x g; 4˚C) and serum was stored at -80˚C.

Where indicated, miR-9-5p mimic (100 μl; 50 mg/kg; 5'-GGUUAUCUAGCUGUAUGA-3'; Thermo Fisher Scientific, Inc., Waltham, MA, USA) or antagomir (100 μl; 50 mg/kg; 5'-AUACAGCUAGAUAACCAAAG-3'; Thermo Fisher Scientific, Inc.) was injected in the liver at 1 h before performing the IR (n=6/group) without anesthesia of rats.

Quantification of cytokines. ELISA kits (MyBiosource; Thermo Fisher Scientific, Inc.) were used to quantify liver function markers, including alanine aminotransferase (ALT; cat. no. MBS1601726), aspartate aminotransferase (AST; cat. no. MBS778086), lactate dehydrogenase (LDH; cat. no. MBS778339) (20), and inflammatory cytokines, including interleukin (IL)-1 (cat. no. MA5-23,736), -6 (cat. no. M620) and -10 (cat. no. AHC0103) and tumor necrosis factor (TNF)-α (cat. no. P300A), in serum following the manufacturer's protocols. Data are presented as the mean ± standard error of mean and experiments were performed three times in triplicate.

Immunoblot analysis. To extract the proteins, liver tissue cells and Hep3B cells were lysed in radioimmunoprecipitation assay buffer (Thermo Fisher Scientific, Inc.) supplemented with Mini protease inhibitor cocktail (Roche Diagnostics, Indianapolis, IN, USA). The protein concentration was determined using bicinchoninic acid kit (Thermo Fisher Scientific, Inc.). Whole cell lysate (50 μg) was separated on 10% SDS-PAGE gels and transferred to polyvinylidene difluoride membranes. Membranes were blocked for 1 h at 25˚C using 4% non-fat milk (Thermo Fisher Scientific, Inc.) and probed with anti-GAPDH antibody (cat. no. ab9458; 1:1,000); anti-phosphorylated (p)-p65 antibody (cat. no. ab76302; 1:500); anti-total p65 antibody (cat. no. ab207297; 1:500); anti-IκBα antibody (cat. no. ab55341; 1:500; all Abcam, Cambridge, UK) at 4˚C for 12 h. Membranes were then incubated with goat anti-rat IgG horseradish peroxidase-conjugated antibody (cat. no. ab205720; 1:2,000; Abcam) for 1 h at 25˚C. Blots were visualized using enhanced chemiluminescence reagent (Thermo Fisher Scientific, Inc.). GAPDH was used to confirm equal loading.

RNA and miRNA extraction and reverse transcription-quantitative polymerase chain reaction (RT-qPCR). TRIzol reagent (Sigma-Aldrich; Merck KGaA, Darmstadt, Germany) was used to isolate total RNA and miRNA from tumor tissues. The SuperScript III First Strand cDNA synthesis kit (Thermo Fisher Scientific, Inc.) was to obtain first strand cDNA using the following protocol: 30˚C for 10 min, 42˚C for 30 min, 99˚C for 5 min followed by 5˚C for 5 min. TaqMan Gene Expression probes (Thermo Fisher Scientific, Inc.) were used for subsequent RT-qPCR assays. TATA-box binding protein was used as normalization control for assessing *NFKB3* transcription levels. Primers sequences were as follows: *NFKB3* forward, 5'-GACGACTGTTCCCCCTC-3' and reverse, 5'-CCTCGCACTTGTAGCGG-3' (21); miR-9-5p forward, 5'-GTGCAGGGTCCGAGGT-3' and reverse, 5'-GCG CTCTTTGGTTATCTAGC-3' (22); *TBP* forward, 5'-CCCGAA ACGCCGAATATAATCC-3' and reverse, 5'-AATCAGTGC CGTGGTTCGTG-3' (23); and *RNU6B* forward, 5'-CTCGCT TCGGCAGCACA-3' and reverse, 5'-AACGCTTCACGAATT TGCGT-3' (24). Thermocycling conditions were as follows: 95˚C for 2 min followed by 45 cycles of 94˚C for 15 sec, 55˚C for 15 sec and 68˚C for 30 sec and final elongation at 72˚C for 5 min. Data was analyzed using the $2^{-\Delta\Delta Cq}$ method (25). TaqMan probe based quantification was done for *RNU6B* and miR-9-5p, where *RNU6B* was the normalization control. *TBP* was used as control for mRNA.

Gene construction, transfection of plasmid constructs and in vitro luciferase reporter assays. The *NFKB3* 3'-untranslated region (UTR) was constructed by amplifying the endogenous *NFKB3* 3'-UTR from the pMirTarget plasmid (OriGene Technologies, Inc., Rockville, MD, USA) and cloning into the pCXCR4 6X *Renilla* luciferase vector (OriGene Technologies, Inc.). The *NFKB3* 3'-UTR miR-9-5p binding mutant (deleted region, 29-35) construct was generated by site-directed mutagenesis. Hep3B cells ($2x10^6$) were transiently transfected with the reporter construct (4 μg) and a control luciferase vector (4 μg) using Lipofectamine 2000 (Thermo Fisher Scientific, Inc.) according to the manufacturer's instructions. Cells were co-transfected with anti-miR-9-5p antagomir (5'-AUACAG CUAGAUAACCAAAG-3'; Thermo Fisher Scientific, Inc.) or antagomir control (cat. no. miR03201-1-10; Guangzhou RiboBio Co., Ltd., Guangzhou, China). Transfection efficiency was determined by RT-qPCR and luciferase activity. Luciferase activities were determined using the Dual-luciferase reporter assay system (Promega Corporation, Madison, WI, USA) and normalized to *Renilla*. Data are presented as the mean in relative fluorescence units ± standard error of mean.

Regulation of p65 using miR-9-5p. In order to explore regulatory effects of miR-9-5p on p65, miR-9-5p antagomir (5'-AUA CAGCUAGAUAACCAAAG-3'), antagomir control, miR-9-5p

mimic (5'-GGUUAUCUAGCUGUAUGA-3') and mimic control (cat. no. miR01201-1-5; Guangzhou RiboBio Co., Ltd.) were designed. miRs (100 nmol/l) were transfected into Hep3B cells ($2x10^6$) using Lipofectamine 2000 (Thermo Fisher Scientific, Inc.) according to the manufacture's protocols. Following 6 h, cell culture medium was changed and cells were cultured for further 48 h. Transfection efficiency was determined by RT-qPCR. Subsequently, western blot assays detecting p65 were performed.

Apoptosis quantification by flow cytometry. Liver tissues of the IR+sevoflurane, the IR and the control groups were collected. Tissues were homogenated into single cell suspension using the mechanical trituration method. Cell viability was determined by Annexin-V/propidium iodide (PI) staining (BD Biosciences, Franklin Lakes, NJ, USA), with Annexin-V^-/PI^- as viable, Annexin-V^+/PI as early apoptotic and Annexin-V^+/PI^+ as late apoptotic cells. Samples were analyzed using a BD Accuri C6 flow cytometer with C6 software (version 1.0.264; BD Biosciences). Data are presented as the means ± standard error of mean representative of three experiments and each performed in triplicate.

TUNEL staining assay. Liver tissues of the IR+sevoflurane, the IR and the control groups were collected, fixed using 4% paraformaldehyde for 24 h at 25˚C and 5 μm frozen sections were prepared. TUNEL immunohistochemistry analysis was performed using the TUNEL Apoptosis Assay kit (Shanghai Yeasen Biotech Co., Ltd., Shanghai, China). First, tissue slides were deparaffinized twice for 10 min at room temperature using xylene and treated with proteinase K (20 μg/ml; Sigma-Aldrich; Merck KGaA) for 20 min at 25˚C. Tissue sections were equilibrated in the kit's equilibration buffer (100 μl) for 5 min at 25˚C. FITC-12-dUTP Labeling mix containing recombinant terminal deoxynucleotidyl transferase (100 μl) was added to the sections and samples were incubated at 37˚C in a humidity chamber (plastic box with PBS) for 1 h. Sections were incubated with DAPI at 25˚C for 5 min. Samples were imaged using a fluorescence microscope (magnification, x400) and five random fields were selected for each sample.

Statistical analyses. Statistical analyses were performed using SPSS 20.0 (IBM Corp., Armonk, NY, USA). Differences between groups were determined by one-way analysis of variance followed by least significant difference post-hoc tests. Student's t-test or Mann-Whitney U tests were used for the comparison of two groups. $P<0.05$ was considered to indicate a statistically significant difference.

Results

Sevoflurane reverses IR-induced liver damage in tissues. Liver damage induced by IR was visualized using H&E staining and was graded using the Suzuki score. Pathological changes evident in the IR group indicated severe liver damage and were validated by high Suzuki scores (Fig. 1A and B). Sevoflurane administration significantly attenuated liver damage compared with the IR group ($P<0.01$; Fig. 1A and B). High serum levels of AST, ALT and LDH, indicative of severe liver damage, were observed in the IR group and levels were significantly decreased in the IR+sevoflurane compared with the IR group ($P<0.01$; Fig. 1C-E).

Sevoflurane administration attenuates IR-associated cytokine storms and apoptosis. Levels of inflammatory cytokines were determined in the various experimental groups to evaluate if sevoflurane attenuates IR-associated cytokine storms. Compared with the sham group, TNF-α, IL-1 and -6 levels were significantly increased in the IR group ($P<0.01$; Fig. 2A-C). Sevoflurane administration significantly decreased cytokine levels compared with the IR group ($P<0.01$; Fig. 2A-C). IL-10 levels were significantly reduced in the IR compared with the sham group and this decrease was significantly reversed in the IR+sevoflurane group ($P<0.01$ Fig. 2D). Additionally, TUNEL staining assays and flow cytometry suggested that the late apoptotic rate in the IR group was significantly increased compared with the sham group and sevoflurane significantly attenuated IR-induced late apoptotic rates ($P<0.01$; Fig. 3A-C).

Sevoflurane administration attenuates IR-associated injury via the NF-κB signaling pathway. Activation of the NF-κB signaling pathway was investigated to evaluate if cytokine levels were mediated by this pathway. Levels of total p65 and p-p65 were increased in the IR group compared with the sham group and IκBα, an inhibitor of NF-κB signaling, levels were downregulated (Fig. 3D). Sevoflurane administration increased IκBα expression and decreased total and phosphorylated p65 levels compared with the IR group (Fig. 3D). The results indicated a successful attenuation of NF-κB signaling was detrimental in the protective role of sevoflurane against IR-associated injury and tissue damage.

miR-9-5p affects p65 levels by targeting NFKB3. To explore the mechanism by which p65 levels decreased following IR, miRNA targets were investigated, as no obvious changes in mRNA expression were detected (data not shown). miR-9-5p was predicted as a putative miRNA targeting *NFKB3*, encoding for p65, by TargetScan (Fig. 4A). *NFKB3* mRNA expression was significantly upregulated following IR and miR-9-5p was downregulated in IR tissues compared with the sham control (Fig. 4B and C). Following sevoflurane treatment, *NFKB3* mRNA expression was downregulated while miR-9-5p expression was upregulated in hepatic tissue specimens compared to the IR specimen (Fig. 4D).

To evaluate if *NFKB3* is a direct target of miR-9-5p luciferase reporter assays were performed. Various hepatic cell lines including AML12, HepG2, Hep3B, MIHA, BNL CL.2 and Huh7 were screened for miR-9-5p and *NFKB3* expression and Hep3B exhibited high miR-9-5p and increased *NFKB3* expression compared with these other hepatic cell lines (data not shown). Hep3B cells have previously been used to mimic IR by hypoxia/reoxygenation treatment (26). Hence, Hep3B was selected for subsequent *in vitro* assays. Luciferase reporter constructs containing the wild type *NFKB3* 3'-UTR were transfected with or without the antagomir targeting miR-9-5p. The relative activity in wild type *NFKB3* 3'-UTR containing cells was increased 3.09±0.03 fold ($P=0.0073$; Fig. 4E) in the presence of antagomir compared with the antagomir control cells. The specificity of this interaction was confirmed using a

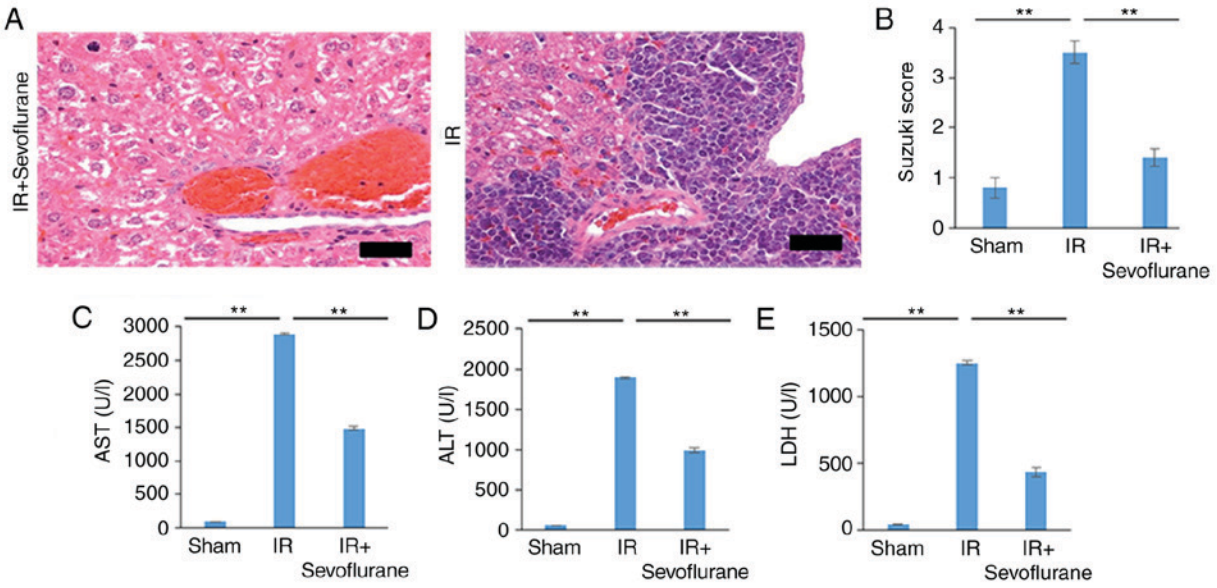

Figure 1. Administration of sevoflurane ameliorates IR-induced liver injury. Rats were randomly divided into the sham, the IR and the IR+sevoflurane groups (n=6 rats/group); the IR groups underwent 1 h ischemia and 2 h reperfusion prior to tissue collection. Rats in the IR+sevoflurane were administered sevoflurane for the duration of the surgery. (A) Representative hematoxylin/eosin staining of liver sections obtained for the IR and the IR+sevoflurane groups (magnification, x200). (B) Suzuki scores determined in tissue specimen. Serum levels of (C) AST, (D) ALT and (E) LDH. Results are expressed as the mean ± standard error of the mean of three independent experiments. **P<0.01. IR, ischemia/reperfusion; AST, aspartate aminotransferase; ALT, alanine aminotransferase; LDH, lactate dehydrogenase.

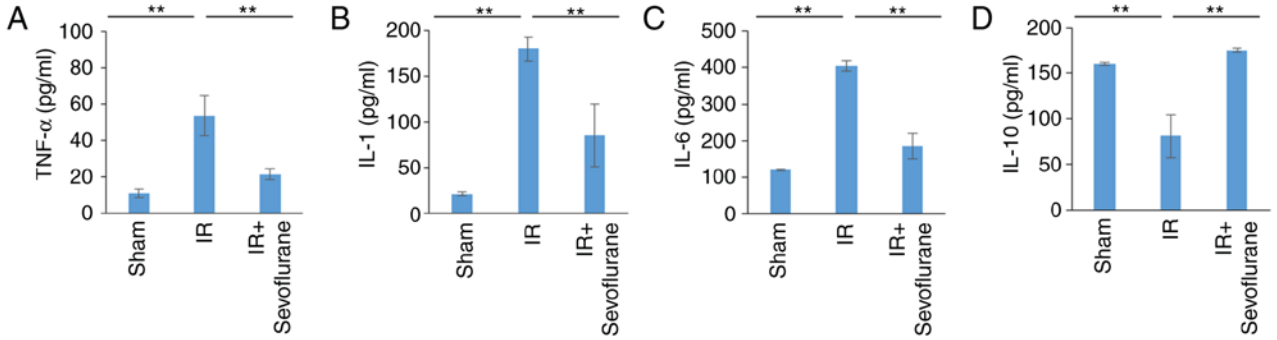

Figure 2. Effects of sevoflurane on IR-induced inflammation in liver tissues. Rats were randomly divided into the sham, the IR and the IR+sevoflurane groups (n=6 rats/group). Animals in the IR groups underwent 1 h ischemia and 2 h reperfusion and rats in the IR+sevoflurane were administered sevoflurane for the duration of the surgery. Serum levels of inflammatory cytokines (A) TNF-α, (B) IL-1, (C) IL-6 and (D) IL-10 were determined. Results are expressed as the mean ± standard error of the mean of three independent experiments. **P<0.01. IR, ischemia/reperfusion; TNF, tumor necrosis factor; IL, interleukin.

miR-9-5p binding mutant of the *NFKB3* 3'-UTR. No significant difference was determined between the anti-miR-9-5p antagomir and the antagomir control cells (Fig. 4E).

Relative miR-9-5p levels were detected in cells transfected with miR-9-5p antagomir, mimic or controls to determine transfection efficiency. miR-9-5p antagomir significantly decreased miR-9-5p levels compared with the antagomir control (P=0.0097) and the miR-9-5p mimic significantly increased miR-9-5p levels compared with the mimic control (P=0.0074; Fig. 4F). Furthermore, p65 expression was increased in the miR-9-5p antagomir compared to control group and decreased in the miR-9-5p mimic compared with the control group (Fig. 4G).

miR-9-5p treatment in rats attenuates IR-induced liver injury. It was further evaluated if protective effects of sevoflurane were mediated by miR-9-5p. Rats of the IR group were injected with miR-9-5p mimic prior to IR induction. Sevoflurane administration and treatment with miR-9-5p mimic significantly attenuated IR-associated liver damage as indicated by the Suzuki score (P<0.01; Fig. 5A). Additionally, decreased AST, ALT and LDH serum levels were observed in the IR+miR-9-5p mimic and the IR+sevoflurane groups compared with the IR group (P<0.01; Fig. 5B-D). Cumulatively, this indicated that protective effect of sevoflurane on IR-associated injury may be mediated miR-9-5p expression.

Sevoflurane alters the NF-κB signaling pathway through miR-9-5p upregulation. To verify whether sevoflurane inhibited NF-κB by upregulating miR-9-5p, western blot analysis investigating p65 phosphorylation and IκBα was performed in the following groups: Sham, IR, IR+sevoflurane, IR+miR-9-5p mimic, IR+miR-9-5p antagomir and IR+sevoflurane+miR-9-5p antagomir. miR-9-5p levels

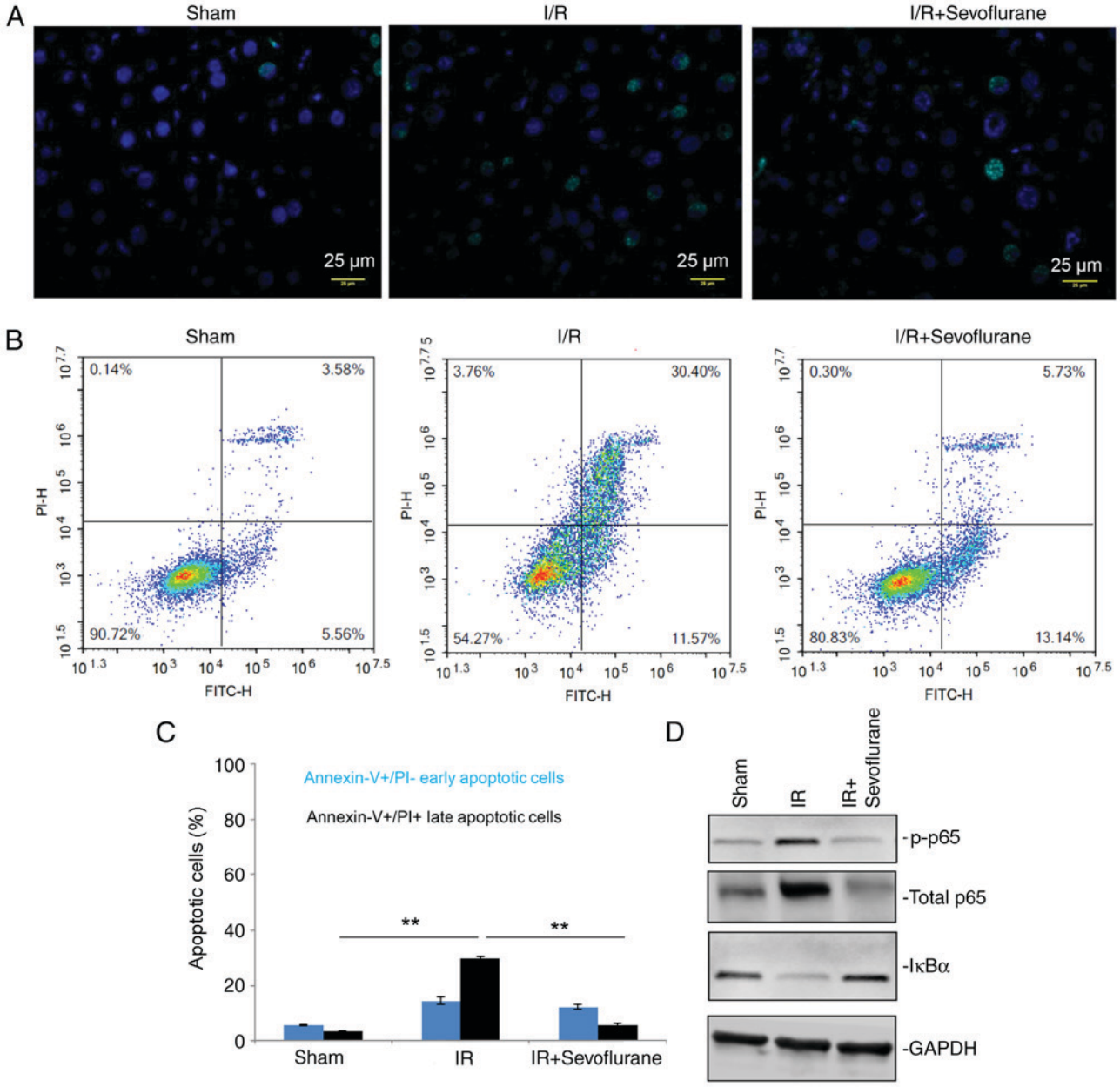

Figure 3. Effects of sevoflurane on apoptosis and NF-κB signaling pathway activation. Rats were randomly divided into the sham, the IR and the IR+sevoflurane groups (n=6 rats/group). Animals in the IR groups underwent 1 h ischemia and 2 h reperfusion and rats in the IR+sevoflurane were administered sevoflurane for the duration of the surgery. (A) Liver tissue sections stained with TUNEL Apoptosis Assay kit (green) and DAPI (blue). (B) Collected liver tissues were homogenated into single cell suspensions for Annexin-V/PI staining. (C) Analysis of the apoptosis rates. Results are expressed as the mean ± standard error of the mean of three independent experiments. (D) Representative western blots p-p65, p65 and IκBα, compared with GAPDH. **P<0.01. IR, ischemia/reperfusion; PI, propidium iodide; FITC, fluorescein isothiocyanate; p-, phosphorylated; NF, nuclear factor; IκBα, inhibitor of κBα.

were detected to determine transfection efficiency; IR significantly decreased miR-9-5p levels compared with the sham group (P=0.029) and miR-9-5p levels were significantly increased in IR+sevoflurane group and IR+miR-9-5p mimic group compared with the IR group (P=0.022 and P=0.013, respectively; Fig. 6A). In the IR+miR-9-5p antagomir and the IR+sevoflurane+miR-9-5p antagomir groups, miR-9-5p levels were not significantly different compared with the IR group (P>0.05; Fig. 6A). Western blot analysis revealed that p65 phosphorylation was increased in the IR compared with the sham group (P<0.01; Fig. 6B and C). Treatment with sevoflurane and miR-9-5p mimic decreased phosphorylation levels of p65 compared with the IR group (P<0.01; Fig. 6B and C). In the IR+miR-9-5p antagomir and the IR+sevoflurane+miR-9-5p antagomir groups, p65 phosphorylation was not significantly different compared with the IR group (Fig. 6B and C). IκBα expression decreased in the IR compared with the sham group and sevoflurane and miR-9-5p mimic treatment significantly reversed the IR-induced change (Fig. 6B and D). The results indicated that sevoflurane inhibited the NF-κB signaling pathway by miR-9-5p upregulation.

Discussion

miRs are 21-23 nucleotide-long noncoding RNAs that regulate gene expression by inhibiting translation, in case of imperfect

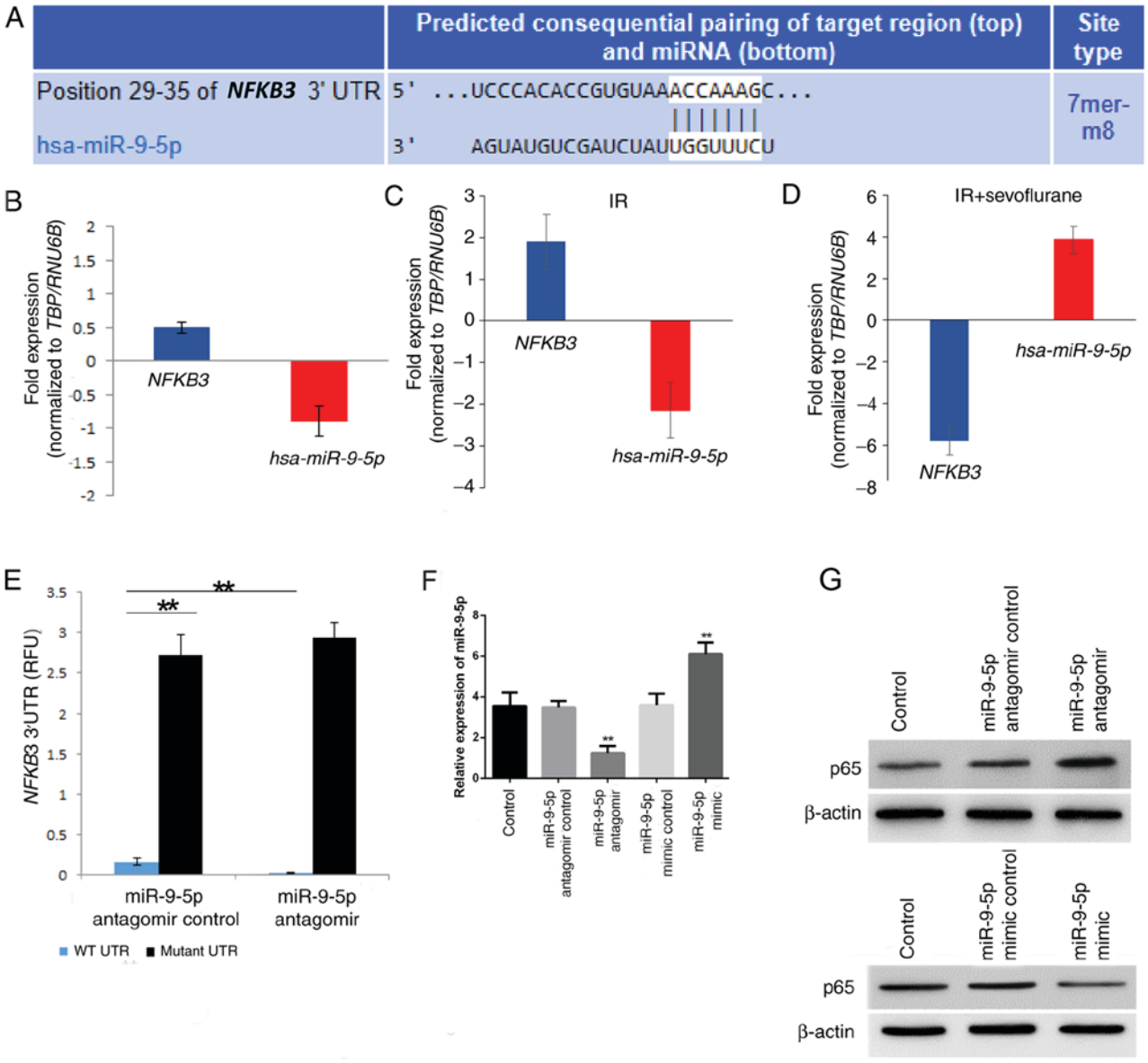

Figure 4. *NFKB3* is a direct target of miR-9-5p. (A) TargetScan predicted a complementary 7mer-m8 seed match between miR-9-5p and the 3'-UTR of *NFKB3*. Relative *NFKB3* and miR-9-5p expression in liver tissues obtained from the (B) sham, (C) IR and (D) IR+sevoflurane experimental groups that underwent 1 h ischemia and 2 h reperfusion and rats in the latter were administered sevoflurane for the duration of the surgery. Results are presented as the mean ± standard error of mean of three independent experiments and data were normalized to *TBP* and *RNU6B* for *NFKB3* and miR-9-5p, respectively. (E) Luciferase reporter activity of WT and mutant *NFKB3* 3'-UTR in the presence and absence of miR-9-5p. (F) Relative miR-9-5p expression and (G) p65 protein expression following transfection of Heb3B with miR-9-5p antagomir, mimic and corresponding controls. Results are presented as the mean ± standard error of the mean of three independent experiments. **P<0.01 vs. Control. IR, ischemia/reperfusion; miR, microRNA; UTR, untranslated region; *NFKB3*, encoding for p65; WT, wild type; TBP, TATA-box binding protein.

complementarity between miR seed the target, or by degrading the target mRNA, in cases of perfect complementarity between the target and miR seed (27,28). miRs are involved in various important physiological processes and in disease pathogenesis (29-34). Sevoflurane is an inhalational anesthetics that is widely used in clinic and has little toxic effects on the liver (35). Low blood pressure and blood loss can lead to organ ischemia during surgery, including of the liver, and IR liver injury is a known side effect (36). Whether sevoflurane exerts protective effects on IR liver injury has not been determined so far.

The current study explored the protective effects of sevoflurane on the IR liver injury in rats and cell models. H&E staining of tissues from various experimental animal groups was performed and Suzuki scores were determined, allowing for the evaluation of the liver injury level. The results demonstrated that sevoflurane protected the structural integrity of the liver in the IR group. Serum markers of liver function, including AST, ALT and LDH, were further determined and supported the conclusion that sevoflurane protected against IR injury. Apoptosis is a result of IR injury. To measure apoptosis in liver tissues, flow cytometry and TUNEL staining assays were performed. The results suggested that sevoflurane inhibited apoptosis rates compared with the IR group. It was presented that sevoflurane protected the function and structural integrity of liver from IR injury.

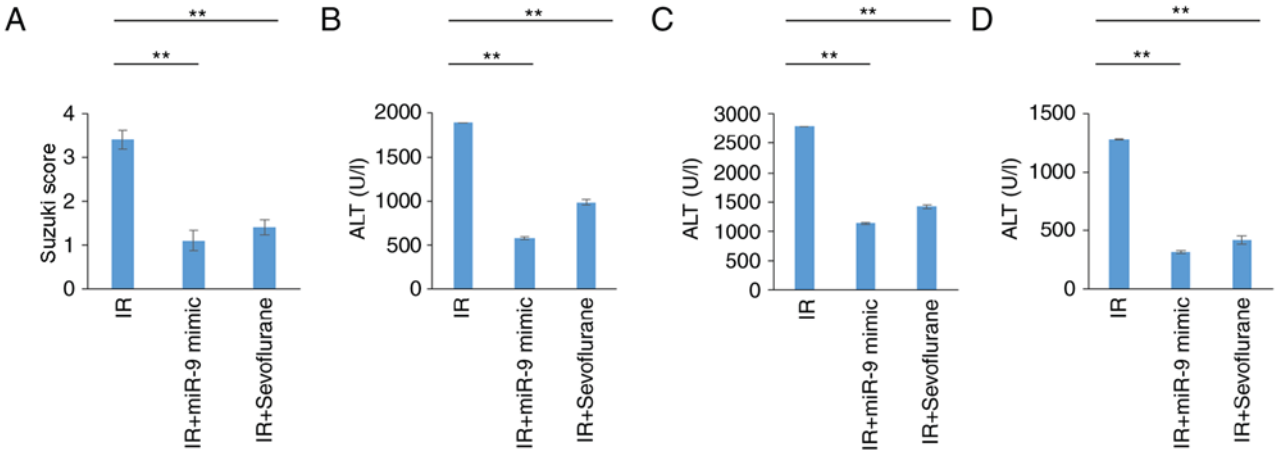

Figure 5. miR-9-5p mimic exerts protective effects similar to sevoflurane in IR-mediated hepatic injury. Rats were randomly divided into IR, IR+sevoflurane and IR+miR-9-5p mimic groups (n=6 rats/group). Animals in the IR groups underwent 1 h ischemia and 2 h reperfusion and rats in the IR+sevoflurane were administered sevoflurane for the duration of the surgery. (A) Suzuki scores determined in the hepatic tissues. Serum levels of (B) ALT, (C) AST and (D) LDH. Results are presented as the mean ± standard error of the mean of three independent experiments. **P<0.01. IR, ischemia/reperfusion; miR, microRNA; AST, aspartate aminotransferase; ALT, alanine aminotransferase; LDH, lactate dehydrogenase.

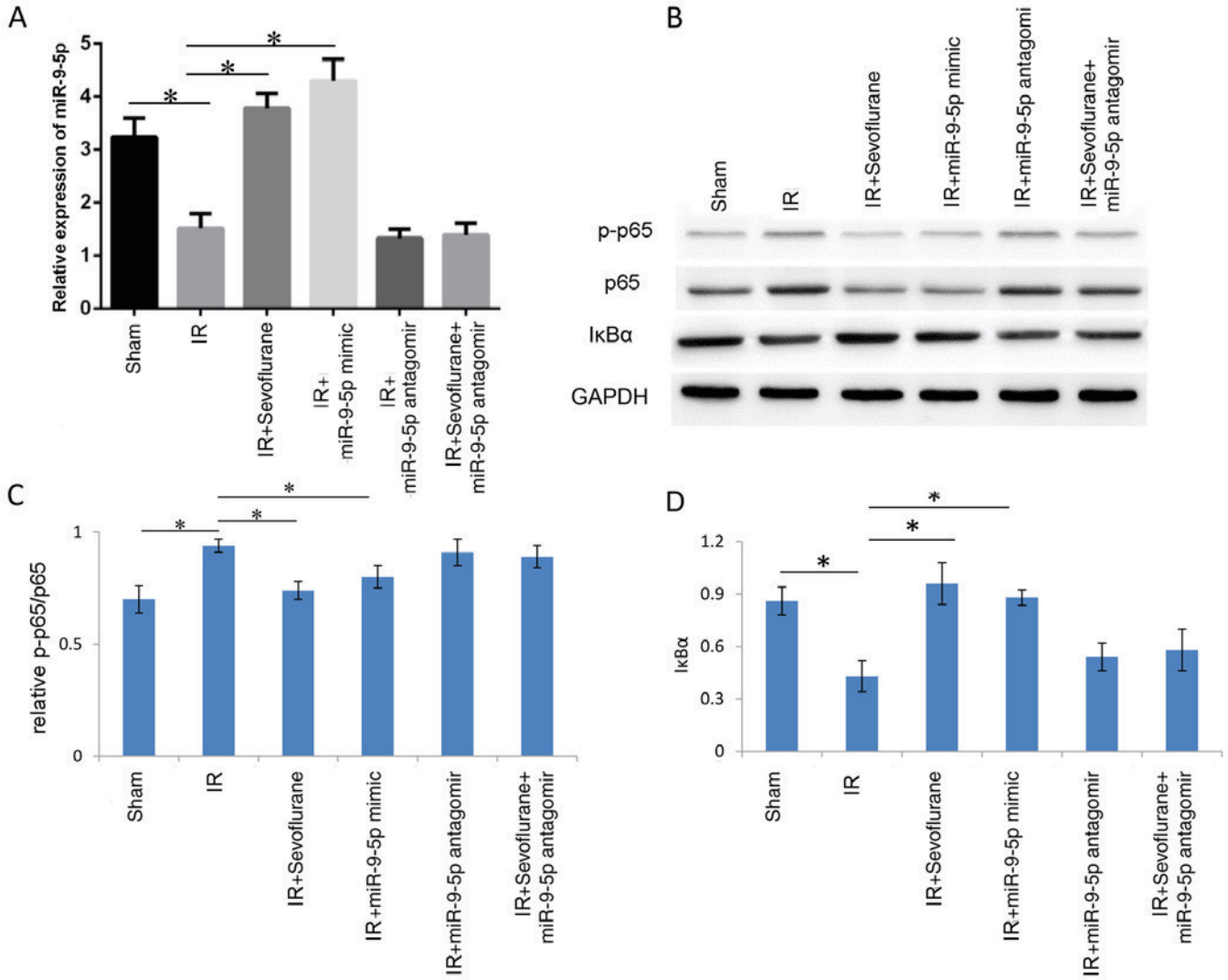

Figure 6. Sevoflurane inhibits the NF-κB signaling pathway through miR-9-5p upregulation. Rats were randomly divided into sham, IR, IR+sevoflurane, IR+miR-9-5p mimic, IR+miR-9-5p antagomir group, IR+sevoflurane+miR-9-5p antagomir groups (n=6/group). The IR+miR-9-5p mimic, IR+miR-9-5p antagomir and IR+sevoflurane+miR-9-5p antagomir groups were injected with miR-9-5p mimic or antagomir in the liver at 1 h prior to IR. (A) Relative miR-9-5p expression. (B) Western blot images for p-p65, p65 and IκBα and quantitative evaluation of (C) p65 phosphorylation and (D) IκBα expression. Results are presented as the mean ± standard error of mean of three independent experiments. *P<0.01. IR, ischemia/reperfusion; miR, microRNA; p-, phosphorylated; NF, nuclear factor; IκBα, inhibitor of κBα.

Inflammation is an important mechanism in IR injury. To explore the protective mechanism of sevoflurane, key inflammation factors were determined in serum samples. TNF-α, IL-1 and IL-6 serve important roles in innate immunological response and IL-10 exhibits negative immunological regulation effects (37). The current study described that IR significantly increased the serum levels of TNF-α, IL-1 and IL-6, and IL-10 was decreased. Following sevoflurane treatment, proinflammatory factors, TNF-α, IL-1 and IL-6, were all decreased and the anti-inflammatory factor IL-10 was increased compared with the IR group. This suggested that sevoflurane inhibited inflammatory effects induced by IR and contributed to the protection against liver injury.

The NF-κB signaling pathway serves an important role in inflammation activation (38). p65 phosphorylation and IκBα levels were determined, which are key proteins of the NF-κB signaling pathway. It was observed that sevoflurane decreased the p65 phosphorylation and increased IκBα expression compared with the IR group. p65 phosphorylation initiates the transcription of various inflammation factors and promotes inflammation activation (38). IκBα inhibits the NF-κB signaling pathway by masking nuclear localization signals of NF-κB-associated proteins and keeping them sequestered in an inactive state in the cytoplasm (39). These results suggested that sevoflurane inhibited the NF-κB signaling pathway.

miRs paricipate in the regulation of various cell signaling pathways. Utilizing bioinformatic, miR-9-5p was identified to target *NFKB3*, the gene coding for p65. A previous study suggested that miR-9-5p regulated NF-κB in ovarian cancer by targeting to *NFKB1* (40); however, there was no evidence that NF-κB was regulated by miR-9-5p in IR as miRs can have various targets in different cells. Monocyte chemotactic protein-induced protein-1 is a target of miR-9-5p in microglia (41). To determine miR-9-5p expression, RT-qPCR was performed. The results suggested that sevoflurane potentiated protective effects by inducing miR-9-5p expression. Hep3B cell treatment with miR-9-5p antagomir increased p65 expression and miR-9-5p mimic significantly decreased p65 expression compared with the respective controls. Furthermore, miR-9-5p mimic exhibited similar protective effects on IR injury as sevoflurane. Results suggested that the volatile anesthetic protected from IR injury by increasing miR-9-5p expression, which in turn directly targeted the proinflammatory NF-κB signaling pathway.

Whether the induction and suppression of miR are direct effects of sevoflurane treatment remains to be investigated. It is imperative that promoter analyses of induced and suppressed miRs are performed to determine which factors are directly regulating expression and how these are manipulated by sevoflurane administration. In addition, the involvement of additional miRs in IR injury and subsequent protection by sevoflurane require to be investigated. There is evidence for the miR-133-5p-mediated regulation of *MAPK6* (42), the miR-182-5p-mediated regulation of *TLR4* (43), the miR-148a-mediated regulation of CamKIIα (44) and the miR-370-mediated regulation of the NF-κB signaling pathway (45) in different aspects of IR injury and amelioration using volatile anesthetics. This indicates that miRs may serve a more important role in IR-associated injury and subsequent remediation by volatile anesthetics.

In conclusion, sevoflurane protected the liver from IR injury by increasing miR-9-5p expression. Increased miR-9-5p expression inhibited NF-κB signaling pathway activation, a cytokine storm and apoptotic cell death. Further research using other models and patients may further the potential clinical administration of sevoflurane to managing IR injury of the liver.

Acknowledgements

Not applicable.

Funding

No funding was received.

Availability of data and materials

The datasets used and/or analyzed during the current study are available from the corresponding author on reasonable request.

Authors' contributions

XL, JZ and ZW contributed to the study design, data acquisition, analysis, statistical analysis and manuscript preparation. SZ contributed to analysis and interpretation of data, and revised the manuscript critically for important intellectual content. All authors read and approved the final manuscript.

Ethics approval and consent to participate

The present study was approved by the Institutional Animal Care and Use Committee of Wuxi People's Hospital Affiliated to Nanjing Medical University.

Patient consent for publication

Not applicable.

Competing interests

The authors declare that they have no competing interests.

References

1. Hochhauser E, Lahat E, Sultan M, Pappo O, Waldman M, Sarne Y, Shainberg A, Gutman M, Safran M and Ben Ari Z: Ultra low dose delta 9-tetrahydrocannabinol protects mouse liver from ischemia reperfusion injury. Cell Physiol Biochem 36: 1971-1981, 2015.
2. Zhang X, Tan Z, Wang Y, Tang J, Jiang R, Hou J, Zhuo H, Wang X, Ji J, Qin X and Sun B: PTPRO-associated hepatic stellate cell activation plays a critical role in liver fibrosis. Cell Physiol Biochem 35: 885-898, 2015.
3. Li C and Jackson RM: Reactive species mechanisms of cellular hypoxia-reoxygenation injury. Am J Physiol Cell Physiol 282: C227-C241, 2002.
4. Jaeschke H: Molecular mechanisms of hepatic ischemia-reperfusion injury and preconditioning. Am J Physiol Gastrointest Liver Physiol 284: G15-G26, 2003.
5. Montalvo-Jave EE, Piña E, Montalvo-Arenas C, Urrutia R, Benavente-Chenhalls L, Peña-Sanchez J and Geller DA: Role of ischemic preconditioning in liver surgery and hepatic transplantation. J Gastrointest Surg 13: 2074-2083, 2009.
6. Wang Y, Shen J, Xiong X, Xu Y, Zhang H, Huang C, Tian Y, Jiao C, Wang X and Li X: Remote ischemic preconditioning protects against liver ischemia-reperfusion injury via heme oxygenase-1-induced autophagy. PLoS One 9: e98834, 2014.

7. Kang JW, Cho HI and Lee SM: Melatonin inhibits mTOR-dependent autophagy during liver ischemia/reperfusion. Cell Physiol Biochem 33: 23-36, 2014.
8. Grossini E, Pollesello P, Bellofatto K, Sigaudo L, Farruggio S, Origlia V, Mombello C, Mary DA, Valente G and Vacca G: Protective effects elicited by levosimendan against liver ischemia/reperfusion injury in anesthetized rats. Liver Transpl 20: 361-375, 2014.
9. Schulz R, Kelm M and Heusch G: Nitric oxide in myocardial ischemia/reperfusion injury. Cardiovasc Res 61: 402-413, 2004.
10. Ren G, Dewald O and Frangogiannis NG: Inflammatory mechanisms in myocardial infarction. Curr Drug Targets Inflamm Allergy 2: 242-256, 2003.
11. Kihara F, Inoue Y, Arima I, Ono M and Masumoto H: Case of Recklinghausen's disease presenting as acute porphyria in the terminal stage. Naika 18: 381-387, 1966 (In Japanese).
12. Dikmen Y, Eminoglu E, Salihoglu Z and Demiroluk S: Pulmonary mechanics during isoflurane, sevoflurane and desflurane anaesthesia. Anaesthesia 58: 745-748, 2003.
13. Goff MJ, Arain SR, Ficke DJ, Uhrich TD and Ebert TJ: Absence of bronchodilation during desflurane anesthesia: A comparison to sevoflurane and thiopental. Anesthesiology 93: 404-408, 2000.
14. Puglisi F, Crovace A, Staffieri F, Capuano P, Carravetta G, De Fazio M, Lograno G, Lacitignola L, Troilo VL, Martines G, *et al*: Comparison of hemodynamic and respiratory effects of propofol and sevoflurane during carbon dioxide pneumoperitoneum in a swine model. Chir Ital 59: 105-111, 2007.
15. Kim JW, Kim JD, Yu SB and Ryu SJ: Comparison of hepatic and renal function between inhalation anesthesia with sevoflurane and remifentanil and total intravenous anesthesia with propofol and remifentanil for thyroidectomy. Korean J Anesthesiol 64: 112-116, 2013.
16. Erturk E, Topaloglu S, Dohman D, Kutanis D, Beşir A, Demirci Y, Kayir S and Mentese A: The comparison of the effects of sevoflurane inhalation anesthesia and intravenous propofol anesthesia on oxidative stress in one lung ventilation. Biomed Res Int 2014: 360936, 2014.
17. Wu Y, Gu C and Huang X: Sevoflurane protects against hepatic ischemia/reperfusion injury by modulating microRNA-200c regulation in mice. Biomed Pharmacother 84: 1126-1136, 2016.
18. Xu Z, Yu J, Wu J, Qi F, Wang H, Wang Z and Wang Z: The effects of two anesthetics, propofol and sevoflurane, on liver ischemia/reperfusion injury. Cell Physiol Biochem 38: 1631-1642, 2016.
19. Suzuki S, Toledo-Pereyra LH, Rodrigyez FJ and Cejalvo D: Neutrophil infiltration as an important factor in liver ischemia and reperfusion injury. Modulating effects of FK506 and cyclosporine. Transplantation 55: 1265-1272, 1993.
20. Veldhuis GJ, Willemse PH, Sleijfer DT, van der Graaf WT, Groen HJ, Limburg PC, Mulder NH and de Vries EG: Toxicity and efficacy of escalating dosages of recombinant human interleukin-6 after chemotherapy in patients with breast cancer or non-small-cell lung cancer. J Clin Oncol 13: 2585-2593, 1995.
21. Sun S, Guo M, Zhang JB, Ha A, Yokoyama KK and Chiu RH: Cyclophilin A (CypA) interacts with NF-κB subunit, p65/RelA, and contributes to NF-κB activation signaling. PLoS One 9: e96211, 2014.
22. Li G, Wu F, Yang H, Deng X and Yuan Y: MiR-9-5p promotes cell growth and metastasis in non-small cell lung cancer through the repression of TGFBR2. Biomed Pharmacother 96: 1170-1178, 2017.
23. He A, Chen Z, Mei H and Liu Y: Decreased expression of LncRNA MIR31HG in human bladder cancer. Cancer Biomark 17: 231-236, 2016.
24. Jiang JJ, Liu CM, Zhang BY, Wang XW, Zhang M, Saijilafu , Zhang SR, Hall P, Hu YW and Zhou FQ: MicroRNA-26a supports mammalian axon regeneration in vivo by suppressing GSK3β expression. Cell Death Dis 6: e1865, 2015.
25. Livak KJ and Schmittgen TD: Analysis of relative gene expression data using real-time quantitative PCR and the 2(-Delta Delta C(T)) method. Methods 25: 402-408, 2001.
26. Teng H, Wu B, Zhao K, Yang G, Wu L and Wang R: Oxygen-sensitive mitochondrial accumulation of cystathionine β-synthase mediated by Lon protease. Proc Natl Acad Sci USA 110: 12679-12684, 2013.
27. Bartel DP: MicroRNAs: Target recognition and regulatory functions. Cell 136: 215-233, 2009.
28. Esquela-Kerscher A and Slack FJ: Oncomirs-microRNAs with a role in cancer. Nat Rev Cancer 6: 259-269, 2006.
29. Aleckovic M and Kang Y: Regulation of cancer metastasis by cell-free miRNAs. Biochim Biophys Acta 1855: 24-42, 2015.
30. Gaur A, Jewell DA, Liang Y, Ridzon D, Moore JH, Chen C, Ambros VR and Israel MA: Characterization of microRNA expression levels and their biological correlates in human cancer cell lines. Cancer Res 67: 2456-2468, 2007.
31. Kumar MS, Lu J, Mercer KL, Golub TR and Jacks T: Impaired microRNA processing enhances cellular transformation and tumorigenesis. Nat Genet 39: 673-677, 2007.
32. Lu J, Getz G, Miska EA, Alvarez-Saavedra E, Lamb J, Peck D, Sweet-Cordero A, Ebert BL, Mak RH, Ferrando AA, *et al*: MicroRNA expression profiles classify human cancers. Nature 435: 834-838, 2005.
33. Guo L, Qiu Z, Wei L, Yu X, Gao X, Jiang S, Tian H, Jiang C and Zhu D: The microRNA-328 regulates hypoxic pulmonary hypertension by targeting at insulin growth factor 1 receptor and L-type calcium channel-alpha1C. Hypertension 59: 1006-1013, 2012.
34. Marques FZ, Campain AE, Tomaszewski M, Zukowska-Szczechowska E, Yang YH, Charchar FJ and Morris BJ: Gene expression profiling reveals renin mRNA overexpression in human hypertensive kidneys and a role for microRNAs. Hypertension 58: 1093-1098, 2011.
35. Safari S, Motavaf M, Seyed Siamdoust SA and Alavian SM: Hepatotoxicity of halogenated inhalational anesthetics. Iran Red Crescent Med J 16: e20153, 2014.
36. Kwan I, Bunn F, Chinnock P and Roberts I: Timing and volume of fluid administration for patients with bleeding. Cochrane Database Syst Rev: CD002245, 2014.
37. Lin RK, Zhang CH, Mu N, Yao QY, Dong SL, Ai QB and Wang QX: Effects of astilbin on the expression of TNF alpha and IL-10 in liver warm ischemia-reperfusion injury. Zhonghua Gan Zang Bing Za Zhi 18: 463-466, 2010 (In Chinese).
38. Liu T, Zhang L, Joo D and Sun SC: NF-κB signaling in inflammation. Signal Transduct Target Ther 2: pii: 17023, 2017.
39. Christian F, Smith EJ and Carmody RJ: The regulation of NF-κB subunits by phosphorylation. Cells 5: pii: E12, 2016.
40. Guo LM, Pu Y, Han Z, Liu T, Li YX, Liu M, Li X and Tang H: MicroRNA-9 inhibits ovarian cancer cell growth through regulation of NF-kappaB1. FEBS J 276: 5537-5546, 2009.
41. Yao H, Ma R, Yang L, Hu G, Chen X, Duan M, Kook Y, Niu F, Liao K, Fu M, *et al*: MiR-9 promotes microglial activation by targeting MCPIP1. Nat Commun 5: 4386, 2014.
42. Hao W, Zhao ZH, Meng QT, Tie ME, Lei SQ and Xia ZY: Propofol protects against hepatic ischemia/reperfusion injury via miR-133a-5p regulating the expression of MAPK6. Cell Biol Int 41: 495-504, 2017.
43. Jiang W, Liu G and Tang W: MicroRNA-182-5p ameliorates liver ischemia-reperfusion injury by suppressing Toll-like receptor 4. Transplant Proc 48: 2809-2814, 2016.
44. Zheng D, He D, Lu X, Sun C, Luo Q and Wu Z: The miR-148a alleviates hepatic ischemia/reperfusion injury in mice via targeting CaMKIIα. Xi Bao Yu Fen Zi Mian Yi Xue Za Zhi 32: 1202-1206, 2016 (In Chinese).
45. Zhu J, Zhu F, Song W, Zhang B, Zhang X, Jin X and Li H: Altered miR-370 expression in hepatic ischemia-reperfusion injury correlates with the level of nuclear kappa B (NF-κB) related factors. Gene 607: 23-30, 2017.